Eurographics/ IEEE-VGTC Symposium on Visualization 2009
H.-C. Hege, I. Hotz, and T. Munzner
(Guest Editors)

Volume 28 (2009), Number 3

Visualization of vessel movements

Niels Willems[1], Huub van de Wetering[1], and Jarke J. van Wijk[1]

[1]Department of Mathematics and Computer Science, Eindhoven University of Technology, The Netherlands

Abstract

We propose a geographical visualization to support operators of coastal surveillance systems and decision making analysts to get insights in vessel movements. For a possibly unknown area, they want to know where significant maritime areas, like highways and anchoring zones, are located. We show these features as an overlay on a map. As source data we use AIS data: Many vessels are currently equipped with advanced GPS devices that frequently sample the state of the vessels and broadcast them. Our visualization is based on density fields that are derived from convolution of the dynamic vessel positions with a kernel. The density fields are shown as illuminated height maps. Combination of two fields, with a large and small kernel provides overview and detail. A large kernel provides an overview of area usage revealing vessel highways. Details of speed variations of individual vessels are shown with a small kernel, highlighting anchoring zones where multiple vessels stop. Besides for maritime applications we expect that this approach is useful for the visualization of moving object data in general.

Categories and Subject Descriptors (according to ACM CCS): Computer Graphics [I.3.3]: Line and Curve Generation—

1. Introduction

Analysis of moving objects occurs in various areas, such as biology, sociology, physics, or transportation. Data of moving objects is often large and complex, and contain fuzzy patterns. Therefore moving objects analysis focuses on finding patterns, such as flocks, migration, or congestion [DWe08]. We focus in this paper on seafaring vessels to visually inspect patterns related to area usage.

Nowadays, moving objects are easily tracked using the Global Positioning System (GPS). In the maritime domain professional vessels are equipped with the Automatic Identification System (AIS) [ITU01], which is an advanced GPS device that broadcasts the vessel's status. This status contains both vessel and trajectory information. Vessel information consists of identification numbers, a name, dimensions, and a type, e.g. passenger ship or tanker. Trajectory information consists of position, time, velocity, course, rate of turn, destination, expected time of arrival, draught, and navigational status, e.g. at anchor, moored, sailing, or fishing. A captain is more aware of the situation around using the status of neighbourhood vessels to prevent collisions.

For surveillance purposes, AIS data is collected using a sensor network and send to operators, such as Coast Guard operators, who search for potential danger. Visual comparison of moving icons of the current situation and map overlays with area usage help them to find outliers. But, these overlays may not exist, therefore we propose a method to extract area usage from historical trajectory data. We focus on two area usages at sea: sea lanes and anchor zones.

Area usage can be computed using kernel density estimation, which convolves points with a kernel, resulting in smoothed data. Blurring the path of movement data does not show the speed of the object along its path, therefore we smooth data by taking speed into account. With a novel multi-scale density visualization different features are revealed at each scale.

This paper is organized as follows. Section 2 describes related work. We introduce maritime terminology in section 3. A density model for movement data is defined in section 4, and visualized in section 5. Using real-world data we explore the capabilities of our method in section 6. Finally, we discuss the benefits, drawbacks, and next steps in section 7.

2. Related work

Moving object data is explored extensively using various approaches, such as displaying raw data, aggregated data, or extracted features [AAe08]. Visual analytic approaches use simple visualizations to explore raw data or aggregated data. Density plots only cope with aggregated data and are visualized in various ways. We propose a convolution method as kernel density estimation, but similar convolution approaches appear in graphics.

In visual analytics, moving object data is often used as source data. Andrienko and Andrienko [AA08b] summarize traffic trajectories by clustering and selection to provide a clear and simple overview of traffic situations on a map. In [AA08a] they propose a method for spatio-temporal aggregation of traffic, which allows the user to explore the usage of a road network at various times simultaneously. Pedestrian trajectories are analyzed in [JFSe07] to find anomalies using a wavelet approach.

A density represents a distribution of data. Kernel Density Estimation (KDE) [Sil92] is a mathematical method that computes density by smoothing data points to reduce sampling artifacts. One of the objectives of KDE is to determine hotspots of data points. The Dutch Hydrographic Office *et al.* [Net04] published an example of accumulated vessel traffic, which is a density plot based on sparse human observations of vessels from an airplane during three years. Despite the small number of observations a global overview is given, but details are too noisy to be useful. A car accident distribution [And07] cannot be represented by only plotting points, because overdrawing results in perceptually wrong estimations of the amount of accidents. In disease syndrome distributions [MRe08] sparse and dense areas are equalized by relating the kernel size to the distance of the k nearest neighbour points. The level of attention of downloaded tiles in Microsoft Virtual Earth is displayed using Hotmap [Fis07], which is a 2D histogram that is implicitly smoothed, since the user always loads neighbouring tiles.

A density D is a function of the form $z = D(x,y)$ and visualized as a 2D height field by a straightforward color map, contour plot, or terrain map. For quantitative analysis, a contour plot is preferred over a color map, since value estimation by colors is perceptually hard. Since contour plots only use isolines, color can be used for other purposes. For a terrain map occlusion problems may occur. In 2D, the density plot becomes visually more attractive by using shading, which can be enriched to a contour map [vWT01].

The convolution computation in KDE is point-based, but convolution along trajectories, or paths, is not well-known in this context. In computer graphics similar computations appear in convolution surfaces and motion blur. A convolution surface is an implicit surface defined by the iso-surface of a convolution around a moving point. By weighing the contribution [JT02] with a polynomial, analytical solutions for non-uniform distributions can be found in a number of cases. A similar convolution along a path appears in motion blur [SPe02], where the luminance is spatially smeared out along paths formed during the shutter time.

3. Terminology and definitions

In this section we briefly introduce geographical, navigational, and maritime terms and definitions.

A position (ϕ,λ) on the earth is specified with *geographical coordinates* latitude ϕ and longitude λ. The coordinates ϕ and λ are given in degrees. Notice that geographical coordinates are independent from the radius of the earth R, which varies in an elliptical shape between 6,357km and 6,378km. For small-scale maps, like ours, (up to 1:5,000,000) the earth can be approximated by a sphere, where large-scale maps require a more complex elliptical model [KK01].

A *map projection* $(x,y) = m(\phi,\lambda)$ maps geographic coordinates to a plane, and often has an inverse m^{-1} [Sny93]. Thousands of map projections with various properties exist. The main properties are preservation of angles (conformal, e.g., Mercator projection M), preservation of distance (equidistant, e.g. equirectangular projection E), and preservation of area (equal area, e.g., sinusoidal projection S). No map projection satisfies all these properties.

The intersection of the earth and a plane through its center is called a great circle, such as the prime meridian or the equator. The *great circle distance* $d_{gc}(\mathbf{p}_0,\mathbf{p}_1)$ is the shortest distance between two points on the earth and is measured along the great circle through these points. Other circles on the earth are small circles.

Vehicles that are not road bound, such as vessels and airplanes, navigate using a compass to move to a destination. From the starting point one moves along a *rhumb line segment* [Ale04], a line segment with a constant compass direction. A rhumb line segment $\widehat{\mathbf{p}_0\mathbf{p}_1}$ is given by a straight line segment equation in a Mercator projection and has length $|\widehat{\mathbf{p}_0\mathbf{p}_1}|$. A natural parametrization $RL(\mathbf{p}_0,\mathbf{p}_1,s)$ between points $\mathbf{p}_i$ for $s \in [0,1]$, is given by a *dead reckoning* [Fav40] principle, which constructs a rhumb line segment starting in $\mathbf{p}_0$ with the same direction as $\widehat{\mathbf{p}_0\mathbf{p}_1}$ and length $s|\widehat{\mathbf{p}_0\mathbf{p}_1}|$. A rhumb line segment may not follow a great circle and hence its path may not be the shortest.

In areas with dense shipping, area usage is established by rules. *Sea lanes* are mandatory for large vessels, with restrictions for draught and direction: high tonnage vessels sail in lanes far from the coast line and lanes are bidirectional but separated. Small vessels have to avoid contact with large vessels, vessels are not allowed to move slowly, and lanes should be crossed perpendicularly. In *anchor zones* vessels drop anchor while waiting for a tug to enter a harbour. Other area usages are oil platforms and wind parks; both should be avoided with reasonable distance during a sea trip.

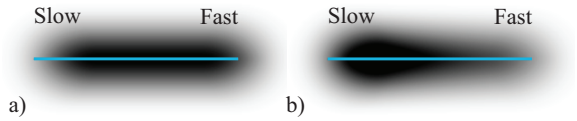

Figure 1: *Convolution. a) At constant speed. b) Accelerated.*

4. Vessel density

This section describes the first part of our method: a model for the contribution of a ship to the density in its neighbourhood as a result of sailing along a trajectory. In section 4.1 a continuous density model is defined. Section 4.2 and 4.3 describe the computation of density from sampled trajectories. In section 4.4, Euclidean space is left for geographical space to compute a geographic density overlay.

4.1. Density

Consider an object o that moves in Euclidean space along a continuous trajectory $\mathbf{p}_o(t)$, for t in time window $[0,T]$. We model the contribution of o at a point $\mathbf{q}$ in its environment, e.g., the duration of o in $\mathbf{q}$. This contribution is modeled with a convolution where the signal at position $\mathbf{r}$ is $\delta(\mathbf{r}-\mathbf{p}_o(t))$ with δ the Dirac delta function, and the response at position $\mathbf{q}$ as a result of the object at position $\mathbf{r}$ is given by the kernel $k(\mathbf{q}-\mathbf{r})$. The contribution at time t at position $\mathbf{q}$ can be written as

$$C_o(\mathbf{q};t) \;=\; \iint_{\mathbf{R}^2} \delta(\mathbf{r}-\mathbf{p}_o(t))k(\mathbf{q}-\mathbf{r})d\mathbf{r}. \qquad (1)$$

Applying the convolution sifting property then simply gives $k(\mathbf{q}-\mathbf{p}_o(t))$ for $C_o(\mathbf{q};t)$. The contribution $C_o(\mathbf{q})$ on point $\mathbf{q}$ taken into account the whole trajectory of o then results from integration over time:

$$C_o(\mathbf{q}) \;=\; \frac{1}{T}\int_0^T k(\mathbf{q}-\mathbf{p}_o(t))dt, \qquad (2)$$

where $\frac{1}{T}$ normalizes the contribution in time to enable comparison of contributions at different time scales. The total contribution of a set of objects O at $\mathbf{q}$ is the sum of all individual contributions:

$$C(\mathbf{q}) \;=\; \sum_{o\in O} C_o(\mathbf{q}). \qquad (3)$$

The contribution sampled with a cell Q can be represented by a density D given by the equation

$$D(Q) \;=\; \rho \iint_Q C(\mathbf{q})d\mathbf{q}, \qquad (4)$$

where ρ is a scaling factor for unit conversion, e.g., from a number of vessels per km^2 to a number of vessels per 1000km^2. The density is often investigated on a logarithmic scale $\log(D(Q)+1)$, to display different orders of magnitude. Figure 1 shows the effect of taking a variable speed into account for convolution along a line.

4.2. Trajectory reconstruction

In real-world data a continuous trajectory $\mathbf{p}(t)$ is irregularly sampled in time resulting in positions $\mathbf{p}(t_0),\mathbf{p}(t_1),\ldots,\mathbf{p}(t_N)$ and velocities $v_i = v(t_i)$ at time t_i. For a reconstruction of the trajectory using these samples, we assume that objects move over a straight line segment between consecutive sample points. For line segment $\mathbf{p}_0\mathbf{p}_1$ with $\mathbf{p}_0 = \mathbf{p}(t_0)$ and $\mathbf{p}_1 = \mathbf{p}(t_1)$, we model the position $x(t)$ on the line segment at time $t \in [t_0,t_1]$ by

$$\mathbf{p}(t) = \mathbf{p}_0 + x(t)\frac{\mathbf{p}_1-\mathbf{p}_0}{||\mathbf{p}_1-\mathbf{p}_0||}, \qquad (5)$$

where $x(t)$ fulfills boundary conditions:

$$x(t_0) = 0 \;\wedge\; x(t_1) = ||\mathbf{p}_1-\mathbf{p}_0||. \qquad (6)$$

We assume that the acceleration is constant, and minimize the following expression on the velocities in the end points:

$$(\dot{x}(t_0)-v_0)^2 + (\dot{x}(t_1)-v_1)^2. \qquad (7)$$

This results in the following quadratic equation for $x(t)$:

$$x(t) = \tfrac{1}{2}a(t-t_0)^2 + v(t-t_0) \qquad (8)$$

where the reconstructed acceleration a and velocity v are

$$a = \frac{v_1-v_0}{t_1-t_0} \;\wedge\; v = \dot{x}(t_0) = \frac{||\mathbf{p}_1-\mathbf{p}_0||}{t_1-t_0} - \frac{v_1-v_0}{2}. \qquad (9)$$

By inverting (8) we find t given the position x if we assume that vessels do neither stop nor return, that is $\dot{x}(t) > 0$:

$$t(x) \;=\; \begin{cases} t_0 - v/a + \sqrt{v^2+2ax}/a, & \text{if } a \neq 0; \\ t_0 + x/v, & \text{if } a = 0. \end{cases} \qquad (10)$$

4.3. Density computation

In this section we discuss methods to compute density. We consider the reconstructed trajectories and focus on the computation of $C_o(\mathbf{q})$ in (2) for a single line segment $\mathbf{p}_0\mathbf{p}_1$ in a point $\mathbf{q}$. If a kernel is independent of position and orientation of the line segment, then the integral becomes invariant under rigid transformation. Without loss of generality the points can be written as

$$\mathbf{p}_0 = (x_0,0) \wedge \mathbf{p}_1 = (x_1,0) \wedge \mathbf{q} = (0,y) \text{ with } y \geq 0 \qquad (11)$$

and the integral reduces to

$$C(\mathbf{q}) \;=\; \frac{1}{T}\int_{t_0}^{t_1} k((-x(t),y))dt. \qquad (12)$$

This integral is numerically approximated. So far we found that a cone kernel suits our needs. For such an isotropic kernel with finite support and radius K where $C(\mathbf{q}) = 0$ for all $\mathbf{q}$ with $||\mathbf{q}|| > K$, the computational costs of $C(\mathbf{q})$ can be reduced, since for a line segment $\mathbf{p}_0\mathbf{p}_1$ partially within distance K of $\mathbf{q}$, tighter integration bounds τ_i exist. Let X be the interval on the x-axis where the distance to $\mathbf{q}$ is at most K. If $X \cap [x_0,x_1] = \emptyset$ the integral is zero, otherwise $X \cap [x_0,x_1] = [a_0,a_1]$ for some a_i and the new integration bounds $\tau_i = t(a_i)$ are given by (10).

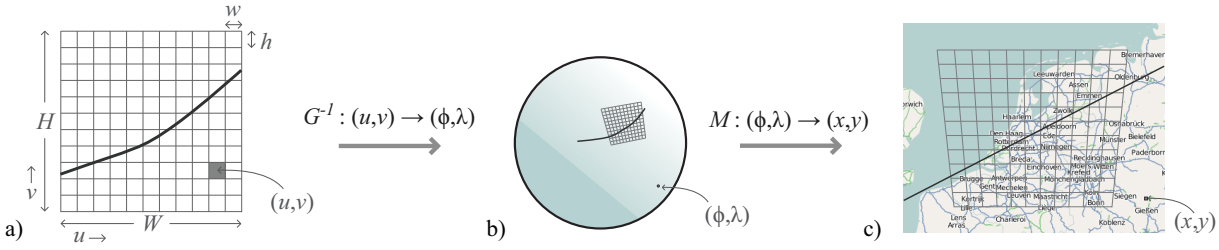

Figure 2: *Computation in various spaces: a) grid space. b) geographic space. c) image space.*

4.4. Geographic implementation

We move from an Euclidian coordinate system to a geographic coordinate system, to investigate movements of objects on the earth, in particular vessels. Density is computed geographically, where we distinguish three kinds of spaces (figure 2): grid space, geographic space, and image space. To compute density using the input data for equal sized cells, we regularly sample at equal distance in grid space, and hence irregularly in λ and ϕ in geographic space. The data and grid are displayed as an image by transforming all geographic coordinates to a map using a map projection.

4.4.1. Rasterization

The density in equation (4) is computed in a grid of cells, which represent equally sized blocks on the earth. An equal area map projection prescribes a relation between positions on the earth and a regular (u,v)-space, such that the area on the earth of a shape in (u,v)-space stays invariant under any translation in (u,v)-space. We use a sinusoidal projection $S^{-1}(u,v)$ [Sny93] defined for meridian λ_0 as

$$\phi = v \tag{13}$$
$$\lambda = \lambda_0 + u/\cos(v). \tag{14}$$

The sinusoidal projection is a combination of great circle angles in the v dimension and small circles in the u dimension. A scaling factor $\sigma(\phi)$ given by

$$\sigma(\phi) = \frac{2\pi R}{360^\circ}\cos(\phi), \tag{15}$$

defines the length on the surface of the earth per degree, along a small circle at latitude ϕ. Notice that for $\phi = 0$, we get the length per degree for a great circle. To get intuitive parameters, the (u,v)-space is scaled horizontally with $w/\sigma(0)$ and vertically with $h/\sigma(\phi)$ resulting in cells of w km wide and h km high. In this space we define a grid of W km wide and H km high. To minimize the distortion of the rectangularity of the cells we introduce a standard parallel ϕ_0 and transpose the center of the grid to the origin. This results in an adapted sinusoidal projection $G^{-1}(u,v)$

$$\phi = \phi_0 + \frac{h}{\sigma(0)}(v - \tfrac{1}{2}H) \tag{16}$$
$$\lambda = \lambda_0 + \frac{w}{\sigma(\phi)}(u - \tfrac{1}{2}W). \tag{17}$$

The sinusoidal projection is chosen for efficiency reasons. Since every cell needs to be projected, the number of expensive function calls, such as trigonometric functions and square roots, needs to be as small as possible. Other common equal-area map projections, such as Bonne, Molleweide, Albers, and Lambert's, are computationally more expensive.

4.4.2. Geographic vessel density

A real-world trajectory of a non-route bound object consists of a sequence of rhumb line segments (see section 3) instead of line segments. The computation of vessel density is implemented in procedure 1. For each rhumb line segment, the density as displayed in equation (2) is computed for all grid cells. For finite-support kernels only the cells in the Oriented Bounding Box (OBB) at distance K to the rhumb line segment need to be considered.

Procedure 1 Vessel density()

```
D ← 0_{H,B} {D becomes zero matrix}
for o ∈ Objects do
  for i ∈ Trajectory segments [0,N) do
    p0 ← p_o(t_i); p1 ← p_o(t_{i+1})
    for (u,v) ∈ OBB at distance K to p̂0p̂1 do
      {Get geographical coordinate of the cell center}
      q ← G^{-1}(u,v)
      {Assign density based on equation (2)}
      D(u,v) ← D(u,v) + C_{p̂0p̂1}(q)
return D;
```

To compute the density of a rhumb line segment $\widehat{\mathbf{p}_0\mathbf{p}_1}$ for cell at position $\mathbf{q}$, we assume the kernel small enough to be considered flat. Therefore the integration in geographic space uses tight integration bounds for $C_o(\mathbf{q})$ in (12) where x_0, x_1, and y are given by

$$x_0 = |\widehat{\mathbf{p}_0\mathbf{p}_k}| \wedge x_1 = |\widehat{\mathbf{p}_k\mathbf{p}_1}| \wedge y = d_{gc}(\mathbf{p}_k, \mathbf{q}). \tag{18}$$

with $\mathbf{p}_k$ on $\widehat{\mathbf{p}_0\mathbf{p}_1}$ with smallest great circle distance to $\mathbf{q}$.

5. Visualization

A density D computed in procedure 1 can be considered as a height field to be visualized on a map using classical car-

tographic methods such as color mapping with a continuous color map (figure 3a) or a discrete color map (figure 3b) which implicitly shows contours. These classical approaches provide an overview of area usage, but the temporal aspect of trajectories disappears in the smoothing. The temporal aspect appears when the data is smoothed with a small kernel, because less interaction between trajectories takes place. Note further that slow vessels produce trajectories with a higher density than fast moving ones, so density provides an indication of the speed.

To get both an overview and a detail view, we separately compute a density D_{large} with a large kernel and a density D_{small} with a small kernel and display them simultaneously in the same area. To speed up the computation, D_{large} is computed on a lower resolution than D_{small} without noticeable loss of features. The density resolutions are synchronized by resampling D_{large} using bilinear interpolation.

Our visualization simultaneously displays both densities by shading the color mapped D_{large} with a height map H of the accumulated densities (figure 3c and 3d). Consider a cell Q, then the color $C(Q)$ is defined as

$$H(Q) = \alpha D_{large}(Q) + \beta D_{small}(Q) \quad (19)$$

$$C(Q) = I_p(H(Q))\, ColorMap(D_{large}(Q)). \quad (20)$$

The intensity of the shading I_p is obtained with Phong illumination [Pho75] of H, using one white light source at infinity. The grid is georeferenced on a map using a map projection. To speed up rendering, corners of a rectangle of cells that are almost flat are map projected and the cells in between are bilinearly interpolated.

6. Real-world data

In this section we explore the capabilities of our method with data from the real world. In the first section we adapt an existing simplification method to reduce the size of data sets with attributed trajectories; in section 6.2 we conduct a number of case studies; in the last section we discuss the advantages of vessel density.

6.1. Trajectory simplification

Depending on the velocity and course, trajectory messages are broadcast up to every 2 seconds resulting in massive data sets. We simplify the trajectories for the position and speed dimensions with an adapted version of the accurate Douglas-Peucker (DP) line simplification algorithm [DP73].

The original DP line simplification removes points within a given position error bound ε. It is a recursive algorithm for a pair of point indices (i, j) that computes an index $k \in [i, j]$ such that $\mathbf{p}_k$ has the largest distance to line segment $\mathbf{p}_i\mathbf{p}_j$ and checks if the distance $d(k,i,j)$ of $\mathbf{p}_k$ to line segment $\mathbf{p}_i\mathbf{p}_j$ is smaller than ε; if so, the line segment is accepted, otherwise the procedure repeats for (i,k) and (k,j). We use this same scheme twice to first accept points based on their speed and subsequently simplify the line segments between the accepted points based on *geographic* coordinates; to do so we vary only the distance function d.

		ε_p (m)		
	(%)	50	100	250
ε_v (knot)	0.5	79.0	80.4	80.8
	1	83.2	84.9	85.3
	5	91.9	94.0	94.8

Table 1: *Amount of ignored data within error ε_p and ε_v.*

A good reconstruction requires points with extreme speed in a simplified trajectory. In the DP scheme the following distance is compared to error ε_v in the speed reconstruction:

$$d(k,i,j) = |\dot{x}_{i,j}(t_k) - v_k| \quad (21)$$

where $x_{i,j}$ is given by (8) after replacing subscript 0 by i and 1 by j. For all resulting accepted point indices (i, j) we spatially simplify the path $\mathbf{p}_i \ldots \mathbf{p}_j$ within error ε_p using the DP scheme but with distance given by

$$d(k,i,j) = d_{gc}(\mathbf{p}_k, \mathbf{r}(k,i,j)) \quad (22)$$

where d_{gc} is the great circle distance and $\mathbf{r}(k,i,j)$ is the simplified position of the object on $\widehat{\mathbf{p}_i\mathbf{p}_j}$ at time t_k:

$$\mathbf{r}(k,i,j) = RL(\mathbf{p}_i, \mathbf{p}_j, \frac{x_{ij}(t_k)}{x_{ij}(t_j)}). \quad (23)$$

with RL the natural parametrization of $\widehat{\mathbf{p}_i\mathbf{p}_j}$ (see section 3).

Table 1 shows the amount of ignored data for one data set of one day consisting of 1460 vessel trajectories. The straight line nature of vessel trajectories yields a reduction of 79% for small errors, while speed reconstruction is preserved.

6.2. Application

We have implemented vessel density in a custom build geographical information system, which allows drawing on an OpenStreetMap map [Ope]. Our prototype is developed in Java with OpenGL (JOGL), and tested on a machine with an Intel Core2 Duo T7300 (2.0 GHz) processor, 2 GB RAM, NVidia Geforce 8600M GT, and Windows Vista (32 bits). Figure 4a can be computed in 10 minutes per day of data, containing 100,000 rhumb line segments, resulting in an overlay of 2000×2000 pixels covering an area of 400×400 km. In this section we apply our method in various use cases.

6.2.1. Weather

The base case is investigation of shipping movement during smooth weather. In figure 3 we show the entrance of Rotterdam harbour, where anchor zones pop up by the highlighted dots of the individual trajectories. On a large scale the same method results in similar patterns. In figure 4a we see that

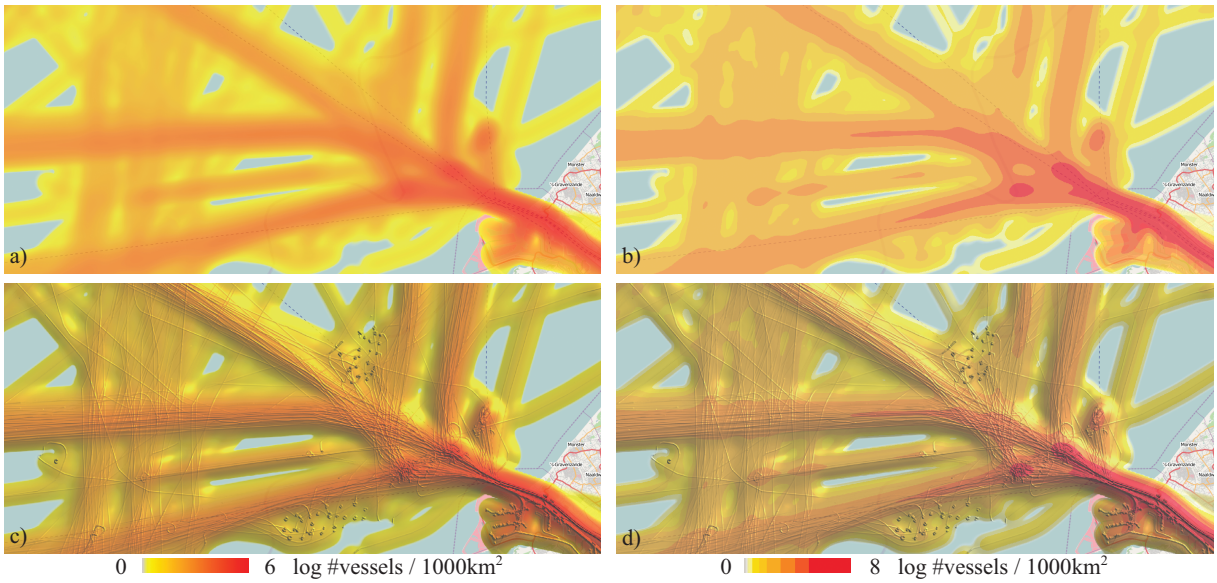

Figure 3: *Vessel density on a logarithmic scale in front of the harbour of Rotterdam, The Netherlands, of a single day convolved with a kernel of 1.5km. The multi-scale density is decorated with convolved trajectories with a kernel of 100m. a) Density with continuous color mapping . b) Density with discrete color mapping. c) Multi-scale density with continuous color mapping. d) Multi-scale density with discrete color mapping.*

three north-south sea lanes appear. Furthermore, some maintenance vessels move slowly in a small area, typically around an oil platform or a wind mill park, which can be observed by the intense individual trajectories. Lastly, in the south the ferry between Vlissingen and Breskens yields regular traffic which can be observed by intense dots just before the sea lane.

Shipping movements differ during a gale. In figure 4b, a northwest gale of force 8 on the scale of Beaufort appears during the day. In general, there are fewer shipping movements and sea lanes are less used compared to figure 3d. Captains try to keep course, but from the twisty individual trajectories we see that they drift slightly. Furthermore, anchor zones are less often used, and vessels slowly sail along the wind towards the anchor zones to avoid rolling, as can be observed by intense left-top to right-bottom trajectories.

6.2.2. Slow movers

Slow movers in sea lanes are not allowed. In this use case we investigate if they appear anyway. In figure 4c the large kernel vessel density is displayed only for trajectory segments where vessels move less than three knot. The density is displayed using a blue-red-blue color map to avoid too much attention to high density. In figure 4c, filtered data of smooth weather is shown and slow movers appear in a sea lane in the lowerleft corner.

6.3. Discussion

A simple approach to compute densities is to convolve trajectories assuming a constant speed of all vessels, whereas in our approach speed is taken into account. In figure 5 these two approaches are compared. We notice three differences when velocity is taken into account. First of all, slow movers are highlighted as shown in the anchor zones. Secondly, the north-south sea lanes differ, which means that the probability to meet a vessel in the right lane is higher than in the left one. Lastly, our model fades distracting, large positional sensor errors as shown in the green box. In the left picture we see a trajectory that is hidden in the transparent lower values of the color map in the right. Since in the reconstruction of the trajectory the begin and end speed are adapted to the distance, the vessel hardly contributes for far erroneous positions.

In general, our density shows speed variations with vessel data, but the slow and steady nature of vessel movements does not result in clear acceleration patterns. However, in other application domains more turbulent data sets exist, such as car, airplane, or mouse trajectories, in which acceleration patterns are expected to show up.

7. Conclusion and Future work

We have presented a novel method to compute and visualize moving objects in such a way that speed is taken into account. In order to do so, we have defined a convolution

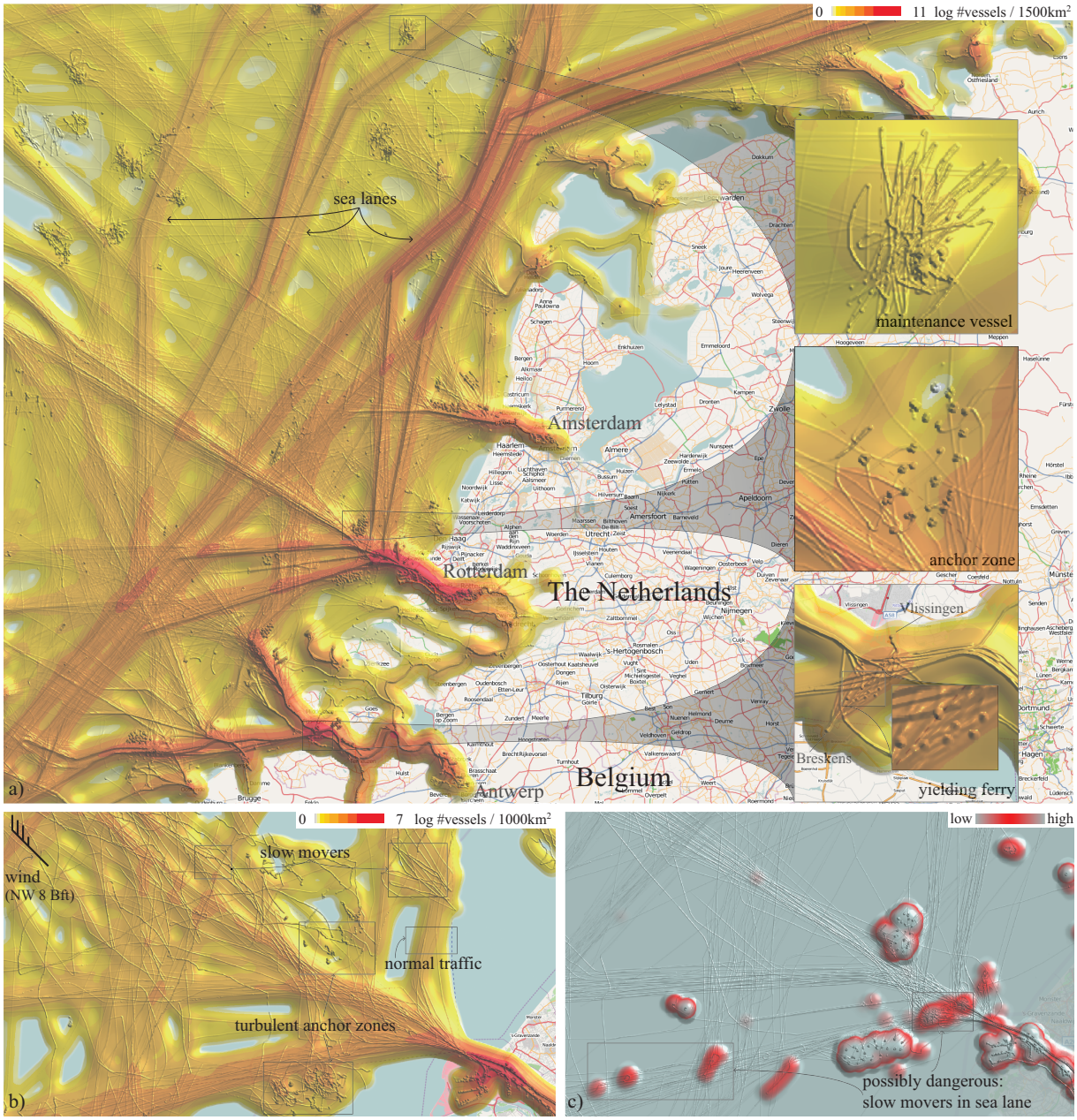

Figure 4: *a) Vessel density of the Dutch coast: Trajectories of a week covering 160,000km^2, and convolved with kernels of 5km and 200m. The picture represents 3.5GB of data. The anchor zone and yielding ferry inset are renderings of a day using kernels of 1.5km and 100m. b) Vessel density of a stormy day: northwest wind with force 8 on the Beaufort scale change the movement pattern of vessels. c) Vessel density of areas where vessels sail less than 3 knot during smooth weather.*

method for a kernel density estimation, which returns the proper contribution per moving point to the overall density. Furthermore, we created an overview + detail visualization using a multi-scale approach for simultaneously displaying two densities with a small and large kernel, which reveal different features. Velocity adapted convolution is applied in the maritime domain showing maritime significant areas such as sea lanes and areas where vessels move slowly or stop. Lastly, our method is applied to weather conditions, which results in heavily changing patterns.

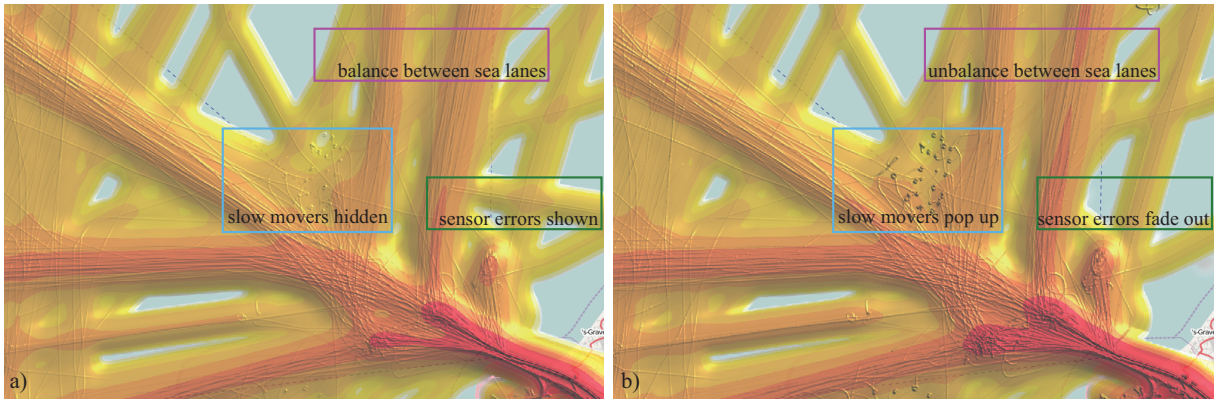

Figure 5: *Comparison of convolution with 15 knot fixed speed (a) and velocity adjusted vessel density (b). The colored boxes annotate some of the visible differences between the convolution methods.*

We are investigating the following problems: Firstly, design of interactive tools for operators to enable comparison of densities for multiple times of day, multiple weather conditions, or multiple ship types, for instance. Secondly, combined visualization of densities and other trajectory attributes such as rate of turn, navigational status, and course. Thirdly, cope with unreliable data: Sensors collecting AIS data may be unavailable resulting in blind spots. Lastly, investigation of movement density in other domains.

Acknowledgements

We thank the reviewers for their comments and thank Thales for their active participation, in particular Hans Hiemstra. This work has been carried out as a part of the Poseidon project at Thales Nederland under the responsibilities of the Embedded Systems Institute (ESI). This project is partially supported by the Dutch Ministry of Economic Affairs under the BSIK program.

References

[AA08a] ANDRIENKO G., ANDRIENKO N.: Spatio-temporal aggregation for visual analysis of movements. *IEEE VAST* (Oct. 2008), 51–58.

[AA08b] ANDRIENKO G., ANDRIENKO N.: *VISUAL 2008*. LNCS 5188. Springer, 2008, ch. A Visual Analytics Approach to Exploration of Large Amounts of Movement Data, pp. 1–4.

[AAe08] ANDRIENKO G., ANDRIENKO N., ET AL.: Geovisualization of dynamics, movement and change: key issues and developing approaches in visualization research. *Information Visualization 7*, 3–4 (2008), 173 – 180.

[Ale04] ALEXANDER J.: Loxodromes: A rhumb way to go. *Mathematics magazine 77*, 5 (Dec. 2004), 349–356.

[And07] ANDERSON T.: Comparison of spatial methods for measuring road accident 'hotspots': a case study of london. *Journal of Maps* (2007), 55–69.

[DP73] DOUGLAS D. H., PEUCKER T. K.: Algorithms for the reduction of the number of points required to represent a digitized line or its caricature. *Cartographica 10*, 2 (Oct. 1973), 112–122.

[DWe08] DODGE S., WEIBEL R., ET AL.: Towards a taxonomy of movement patterns. *Information Visualization 7*, 3–4 (2008), 240 – 252.

[Fav40] FAVILL J.: *Primer of Celestial Navigation*. 1940.

[Fis07] FISHER D.: Hotmap: Looking at geographic attention. *IEEE TVCG 13*, 6 (2007), 1184–1191.

[ITU01] ITU: Technical characteristics for an automatic identification system using time division multiple access in the vhf maritime mobile band. *Recommendation ITU-R M.1371-1* (2001).

[JFSe07] JANOOS, F., SINGH, ET AL.: Activity analysis using spatio-temporal trajectory volumes in surveillance applications. *IEEE VAST* (Nov. 2007), 3–10.

[JT02] JIN X., TAI C.-L.: Analytical methods for polynomial weighted convolution surfaces with various kernels. *Computers & Graphics 26*, 3 (June 2002), 437–447.

[KK01] KENNEDY M., KOPP S.: *Understanding Map Projections*. ESRI Press, 2001.

[MRe08] MACIEJEWSKI R., RUDOLPH S., ET AL.: Contextualizing hotspots - a visual analytics approach. *GIScience* (2008).

[Net04] NETHERLANDS HYDROGRAHIC OFFICE AND MINISTRY OF TRANSPORT, PUBLIC WORKS AND WATER MANAGEMENT: Vessel traffic on the north sea. www.noordzeeloket.nl/Images/VesselTraffic_tcm14-2878.pdf.

[Ope] OPENSTREETMAP:. www.openstreetmap.org.

[Pho75] PHONG B. T.: Illumination for computer generated pictures. *Commun. ACM 18*, 6 (1975), 311–317.

[Sil92] SILVERMAN B. W.: *Density Estimation for Statistics and Data Analysis*. No. 26 in Monographs on Statistics and Applied Probability. Chapman & Hall, 1992.

[Sny93] SNYDER J. P.: *Flattening the Earth: Two Thousand Years of Map Projections*. University of Chicago Press, 1993.

[SPe02] SUNG K., PEARCE A., ET AL.: Spatial-temporal antialiasing. *IEEE TVCG 8*, 2 (Apr.-Jun. 2002), 144–153.

[vWT01] VAN WIJK J. J., TELEA A.: Enridged contour maps. In *IEEE Visualization* (Washington, DC, USA, 2001), pp. 69–74.